

Simultaneous Spectrally and Spatially Resolved Measurements of $3\omega_0/2$ Emission From Laser-Produced Plasmas

P. E. Young, B. F. Lasinski, W. L. Kruer, E. A. Williams, K. G. Estabrook, E. M. Campbell, and R. P. Drake

University of California, Lawrence Livermore National Laboratory, P. O. Box 808, Livermore, California 94550

H. A. Baldis

National Research Council of Canada, Ottawa, Canada

(Received 9 June 1988)

Measurements of three-halves harmonic emission from laser-produced plasmas are presented. The emission from molybdenum targets irradiated with 1.06- μm laser light is simultaneously spectrally and spatially resolved. The data show a clear spatial separation between the blue-shifted and red-shifted components of the three-halves emission. Spectral structure suggests that ion mode coupling is involved in the scattering process.

PACS numbers: 52.35.Mw, 52.40.Db, 52.40.Nk, 52.50.Jm

The two-plasmon decay (TPD) instability¹⁻⁴ is the parametric decay of an electromagnetic wave into two electrostatic waves in the region of the plasma where the electron plasma density n_e is one-quarter of the critical electron density n_c of the incident laser light. The instability has long been of interest both theoretically and experimentally,⁵⁻¹² in part because the electron plasma waves generated by TPD can produce suprathermal electrons which can degrade the performance of inertial confinement fusion targets. The TPD instability has been associated with observations⁶⁻¹¹ of emission at half harmonics of the incident laser frequency, ω_0 . The spectral feature at $3\omega_0/2$ typically appears as a pair of peaks, one blue shifted and the other red shifted with respect to $3\omega_0/2$. Attempts^{6,10} to explain the production of the blue-shifted (red-shifted) component by Raman-type scattering of incident laser photons from TPD plasmons propagating up (down) the density gradient have not adequately explained the angular variation of the relative intensities of the two peaks.

In the experiment reported here, the emission has, for the first time, been simultaneously spatially and spectrally resolved with the result that the blue-shifted feature is observed to originate closer to the target than the red-shifted feature. This is evidence that the blue-shifted (red-shifted) components are associated with TPD plasmons propagating up (down) the density gradient. However, we observe other features, including spectral structure in the emission, which suggest that scattering of the $3\omega_0/2$ photons from ion waves must be considered in order to explain our results.

The experiment used the Phoenix laser facility at the Lawrence Livermore National Laboratory. The laser pulses were of wavelength $\lambda_0 = 1.06 \mu\text{m}$, Gaussian in time with a FWHM of 120 ps, and incident normal to the target. The targets were thick molybdenum slabs which did not burn through during the laser pulse. Dur-

ing the experiment, the $3\omega_0/2$ emission was observed (in the plane of the laser polarization) by imaging the target edge-on through a $\frac{1}{2}$ -m Czerny-Turner spectrometer onto a two-dimensional, optical multichannel analyzer (OMA); data were obtained at many spot sizes and incident laser energies.

The optical system is composed of an $f/5$, 250-mm focal length lens followed by an $f/1.9$, 50-mm focal length relay lens; the magnification of the system is 12.7 and the resolution is $10 \mu\text{m}$. The object plane of the imaging system is chosen to be at the center of the incident laser beam. An alignment pin is used to focus the imaging system and to align the incident laser beam (which is imaged at the target plane in transmission) to the same point. The major alignment error occurs in the focusing of the $3\omega_0/2$ imaging system and is within the depth of focus of the imaging lens ($\pm 50 \mu\text{m}$). The entrance slit of the spectrometer is aligned collinear to the laser axis. The target is backlit with a $3\omega_0$ probe beam which appears in second order at the OMA as a $3\omega_0/2$ wavelength fiducial. Measurement of the FWHM of this line shows that the spectral resolution is limited by the crosstalk of the OMA channels to approximately 0.4 \AA . Some smearing of the image will occur because the OMA records a time-integrated picture of the emission which moves with time, but the smearing is limited by the use of short laser pulses.

Typical data are presented here for a spot size of $100 \mu\text{m}$ and an intensity of $3 \times 10^{15} \text{ W/cm}^2$, which are comparable to the parameters in Refs. 6 and 9. Spectral features upshifted and downshifted from the center frequency are observed (see Fig. 1) with the upshifted component coming closest to the original target surface. If we separately sum over wavelength for both the shifted features seen in Fig. 1, and plot as a function of space, we confirm that the peak emission for the two features are separated by $20 \mu\text{m}$. Since the collecting optic is an

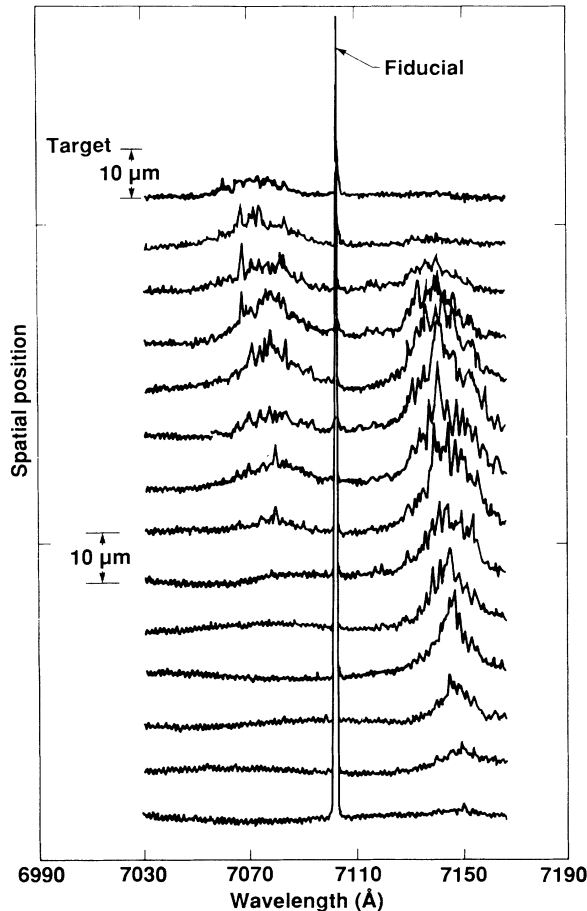


FIG. 1. Plot of the spectral data vs spatial position. The peak at $3\omega_0/2$ is a wavelength fiducial. Note that there is clearly a region where there is a red-shifted feature but no blue-shifted feature.

$f/5$ lens, the object plane would have to be offset ~ 200 μm from the laser axis to produce the observed spatial separation if the red and blue photons were originating from the same point on the side of the plasma opposite the lens. On two occasions separated by six months, we reconstructed and aligned the optical system and obtained similar data; we interpret this to mean that random alignment error is relatively small. Later in this Letter we will consider refraction effects on the photon propagation and find that they cannot explain our observations.

We also see two interesting features which are not sensitive to refraction or alignment. First, we observe a large spatial extent of the red-shifted component (150 μm) away from the target. We will show later that it is difficult to explain the propagation of TPD plasmons to the observed extent of the emission. Second, the data in Fig. 1 also show the presence of spectral structure in both components. The structure in the red-shifted peak in particular often appears to be periodic in wavelength.

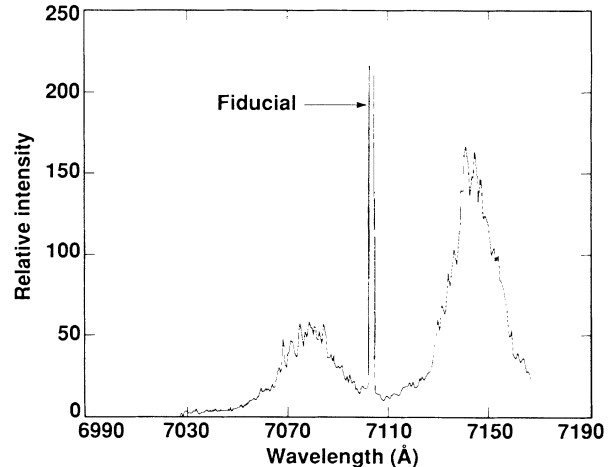


FIG. 2. The data in Fig. 1 have been averaged over space to give an integrated spectrum. Note that the wavelength shift of the peak of the red-shifted feature is slightly larger than that of the blue-shifted feature.

Similar structure has been observed in CO_2 laser plasmas¹² where the TPD plasmon k 's are much larger than the laser wave number k_0 . Previous experiments (with $\lambda_0 \leq 1$ μm) have integrated the light over the entire plasma volume and have observed no structure. Figure 2 (which is a sum over space of the data in Fig. 1) shows that the structure is substantially reduced when integrated over the entire plasma.

In order to interpret our results, we need to model the electron temperature and density profile. The production of plasmas by intense, short laser pulses has been investigated both theoretically^{13,14} and experimentally^{15,16}; these plasmas are composed of a low-density, high-temperature component and a high-density, low-temperature component. It is necessary to invoke a two-temperature plasma in order for significant densities to move 150 μm during the laser pulse. A single-frame interferometer was used on each shot, and although the probe beam pulse (100 ps) is too long to resolve fringes, it has confirmed that the lowest densities of the plasma are expanding at $\sim 3 \times 10^8$ cm/s (corresponding to a low-density expansion driven by a suprathermal electron component with $T_{e,\text{hot}} \sim 30$ keV). From Ref. 14 we estimate that the density of the high-temperature plasma is $\sim 0.05n_c$. We have used the LASNEX¹⁷ fluid code to model the electron temperature and the density profile of the cold plasma component, and find that at $n_c/4$, T_e is ~ 2 keV, which gives a sound speed of $c_s = (ZT_e/M)^{1/2} = 3.1 \times 10^7$ cm/s (for $Z/M = 0.5$). The distance that $n_c/4$ moves is $\sim c_s \tau$ (where τ is the laser pulse length) ≈ 50 μm ; this is consistent with the location of the maximum intensity of both of the peaks of the $3\omega_0/2$ emission. Also, since $c_s \tau <$ the laser spot diameter, the plasma can be considered to be one dimensional (1D). The local plasma-density-gradient scale length L (~ 35 μm)

predicted by LASNEX is consistent with being above the predicted TPD threshold⁴: $k_0 L v_0^2 / v_e^2 = 0.0505 L_\mu \lambda_\mu I_{14} / T_{\text{keV}} > 3$ where $v_e = (T_e / m_e)^{1/2}$ is the electron thermal velocity, $v_0 = eE_0 / m_e \omega_0$ is the electron quiver velocity, L_μ and λ_μ are the scale length and laser wavelength in microns, I_{14} is the laser intensity in units of 10^{14} W/cm², and T_{keV} is the electron temperature in keV.

Next, we will find that Raman-type scattering production of $3\omega_0/2$ photons cannot adequately predict the observations of this experiment (as well as those of previous experiments). First, we calculate the growth rate γ of the TPD plasmons as a function of the plasmon k using Eq. (51) of Ref. 4 (for $\beta \ll 1$) for an inhomogeneous plasma:

$$-\gamma = (1/2\beta^{1/2})(1 - 2\beta q) - 1/2\alpha q^{1/2}\beta^{1/2},$$

where $q = (k_y/k_0)^2$, $\beta = 9v_e^4/v_0^2c^2$, $\alpha = 8\pi(v_0/c)(L/\lambda_0)$, and k_y is the component of the plasmon k perpendicular to k_0 . For the parameters of this experiment, we calculate a broad range of k_y 's ($0.1 < k_y/k_0 < 1.0$) with similar γ 's; the maximum growth rate occurs for $k_y = \pm 0.4k_0$. The component of the plasmon k parallel to k_0 is given approximately by⁴ $k_x = (k_0/2)\{[1 + 4(k_y/k_0)^2]^{1/2} \pm 1\}$. For maximum growth rate, the inward-propagating blue plasmon has $k_1 \approx 1.2k_0$, while the outward-propagating red plasmon has $k_2 \approx 0.5k_0$.

Once the TPD plasmons are created, they must propagate through the plasma until they can k match with photons of frequency ω_0 to produce photons near a frequency of $3\omega_0/2$ in a Raman-type scattering process,^{5,6} i.e., $k^2 = k_0^2 + k_{3/2}^2 - 2k_0k_{3/2}\cos\theta$ where θ is the angle between \mathbf{k}_0 and $\mathbf{k}_{3/2}$, and $k_{3/2} = (3\omega_0/2c)(1 - 4n/9n_c)^{1/2}$. As the plasma wave propagates towards higher densities, the wave-number component k_x decreases and goes to zero at the reflection point. This means that the magnitude of the fastest growing plasmon, for example, is never large enough to directly produce sidescattered ($\theta = 90^\circ$) photons. Even if we consider the entire range of k_y 's, calculated above, that can produce significant TPD growth, we can at most (neglecting momentarily the k -matching condition) get a scattering angle of 45° . From the analysis of Ginzburg,¹⁸ the reflection point for $3\omega_0/2$ photons occurs at a density $n/n_c = \frac{2}{3}[1 - (1 - 4n_0/9n_c)\sin^2\theta]$ where n_0 is the density at which the photons originate. Photons originating at $n_c/4$ with $\theta = 45^\circ$ have a turning point at $n = 1.25n_c$; some of these photons might exit from the plasma within the collection angle of the lens (5.7°) if their turning point is near the edge of the plasma. However, these photons will be refracted between the object plane and the lens, and when projected back to the object plane, will appear to be coming from behind the target surface; instead, the blue-shifted emission peaks $50 \mu\text{m}$ in front of the target.

The red-shifted feature appears to extend to densities which are too low to allow propagation of the TPD plasmons. The distance that the downward-propagating

plasmon can travel is limited by Landau damping. If we neglect $k\lambda_D$ at $n_c/4$, the plasmon dispersion relation can be used to relate the change in $k\lambda_D$ to the change in density down the profile: $\Delta n/n_c = \frac{3}{4}\Delta(k\lambda_D)^2$. As a sample calculation, for $k\lambda_D \approx 0.3$, we calculate the minimum allowed density to be $(n/n_c)_{\text{min}} \approx 0.18$ which is significantly larger than the inferred density of $0.05n_c$ at the outer extent of the observed red component. LASNEX predicts that the distance between 0.25 and $0.18n_c$ is $< 10 \mu\text{m}$ at the end of the laser pulse, so even if $T_e = 4$ keV, then $0.18n_c$ must be less than $100 \mu\text{m}$ from the target. If the observed extent were due to an error in focusing, the error would have to be $\sim 750 \mu\text{m}$ to account for the $75\text{-}\mu\text{m}$ extent of the red component from the peak emission to the lower-density cutoff. If there were an alignment error of this size, we would expect to see a much larger separation of the red and blue components.

The presence of emission from low densities and spectral structure in this experiment, and the observation of sidescattered blue-shifted light in this and other experiments might be explained if the observed $3\omega_0/2$ photons have scattered off ion fluctuations in the plasma. Scattering from ion waves in the three-halves emission process has been investigated in the past^{19,20} and would provide a mechanism by which the scattered photon wave numbers could be changed substantially without significantly changing the photon frequency. This mechanism allows a wider density range for the $3\omega_0/2$ emission since Landau damping does not limit the propagation distance of the photons. Although one might wonder if substantial scattering can occur at very low densities, the observed emission does decrease by a factor of 100 over a density change from 0.25 to $0.05n_c$. Since most of the scattering and absorption of the blue peak (either plasmons or photons) occurs at $n > n_c/4$, fewer photons (relative to the red-shifted photons) remain to be rescattered at $n < 0.18n_c$.

We note that enhanced ion turbulence seeded by hot electrons has been observed in simulations¹⁶ of two-temperature plasmas such as the one reported here. Also Barr and Chen²⁰ have considered modulation of the plasma-wave frequency by ion waves driven by stimulated Brillouin scattering which have $k_i \approx 2k_0$. Using the wavelength of the spectral structure ($\sim 3.3 \text{ \AA}$) we can estimate the k of the ion wave from the dispersion relation $\omega_i = k_i(c_s - u)$, where u is the expansion velocity. From the LASNEX-predicted velocity profile, we take $u \sim 1.5c_s$ and find that $k_i \sim k_0$; this is consistent with the magnitude of k_i required to sidescatter the $3\omega_0/2$ photon.

A 2D expansion of the plasma does not explain either the extent of the red component or our observation of spectral structure. As we noted earlier, the plasma expansion of the low-temperature component should be 1D. We further note that in a 1D plasma of finite extent, the refraction angle α of a directly sidescattered $3\omega_0/2$ pho-

ton is given by²¹ $\alpha = 0.22(n_e/n_c)(l/L)$ rad; a photon originating at $0.3n_c$ (which is above the turning point for the TPD plasmons) at the laser axis will travel a distance $l = 50 \mu\text{m}$ and be refracted by $\alpha = 5.3^\circ$ (assuming $l = 35 \mu\text{m}$) which is within the collection angle of the imaging lens.

In conclusion, we have shown that the two components of three-halves emission are separated in space, an observation which is consistent with photon scattering from TPD plasmons as the source of the $3\omega_0/2$ emission. We find that ion wave scattering of the three-halves photons can qualitatively explain these observations: (1) sidescattered blue photons, (2) red photons originating from low densities, and (3) spectral structure in both components. Further work needs to address the origin of the ion waves responsible.

We thank J. Swain, P. Solone, and W. Cowens for providing laser support during this experiment. Mechanical support was provided by T. Schwinn. This work was performed under the auspices of the U.S. Department of Energy by the Lawrence Livermore National Laboratory under Contract No. W-7405-Eng-48.

¹C. S. Liu and M. N. Rosenbluth, Phys. Fluids **19**, 967

(1976).

²A. I. Avrov *et al.*, Zh. Eksp. Teor. Fiz. **72**, 970 (1977) [Sov. Phys. JETP **45**, 507 (1977)].

³E. Z. Gusakov, Pis'ma Zh. Tekh. Fiz. **3**, 1219 (1977) [Sov. Tech. Phys. Lett. **3**, 504 (1977)].

⁴A. Simon *et al.*, Phys. Fluids **26**, 3107 (1983).

⁵S. J. Kartunnen, Lasers Part. Beams **3**, 157 (1985).

⁶R. E. Turner *et al.*, Phys. Fluids **27**, 511 (1984).

⁷W. Seka *et al.*, Phys. Fluids **28**, 2570 (1985).

⁸F. Amiranoff *et al.*, Phys. Fluids **30**, 2221 (1987).

⁹P. D. Carter *et al.*, Phys. Rev. Lett. **44**, 1407 (1980).

¹⁰V. Aboites *et al.*, Phys. Fluids **28**, 2555 (1985).

¹¹R. W. Short *et al.*, Phys. Rev. Lett. **52**, 1496 (1984).

¹²H. A. Baldis and C. J. Walsh, Phys. Fluids **26**, 1364 (1983); D. M. Villeneuve *et al.*, Phys. Fluids **28**, 1454 (1985).

¹³B. Bezzerides *et al.*, Phys. Fluids **21**, 2179 (1978).

¹⁴M. True *et al.* **24**, 1885 (1981).

¹⁵A. Ehler, J. Appl. Phys. **46**, 2464 (1975).

¹⁶P. Campbell *et al.*, Phys. Rev. Lett. **38**, 1397 (1977).

¹⁷G. D. Zimmerman and W. L. Kruer, Comments Plasma Phys. Controlled Fusion **2**, 51 (1977).

¹⁸V. L. Ginzburg, *The Propagation of Electromagnetic Waves in Plasmas* (Pergamon, New York, 1964), p. 255.

¹⁹A. B. Langdon *et al.*, Phys. Rev. Lett. **43**, 133 (1979); S. J. Kartunnen, Phys. Rev. A **23**, 2006 (1981).

²⁰H. C. Barr and F. F. Chen, Phys. Fluids **30**, 1180 (1987).

²¹F. Jahoda and G. Sawyer, in *Methods of Experimental Physics*, edited by L. Marton (Academic, New York, 1971), Vol. 9B, p. 22.